Azimuth Angle Resolution Improvement Technique with Neural Network

Hyungju Kim, Sungjin You, Byung Jang Jeong, Woojin Byun
Radio & Satellite Research Division
ETRI
Daejeon, Korea
kimhyungju@etri.re.kr, sjyou@etri.re.kr, bjjeong@etri.re.kr, wjbyun@etri.re.kr

***Abstract*— This paper introduces a method to improve the azimuth angle resolution using MIMO-FMCW radar. When using a MIMO-FMCW radar, a 2D radar image composed of a range axis and an azimuth axis can be obtained. The range resolution is determined by the bandwidth, and the azimuth resolution is determined by the length of the virtual antenna array and the number of virtual antenna elements. To improve the azimuth angle resolution while avoiding aliasing, in this paper, the virtual antenna was placed wider with non-uniform spacing. Then, deep learning technique was applied to reduce the side lobe effect. The proposed method was verified through experiments using simulation signals and emulation signals based on measurements.**

Keywords—MIMO-FMCW radar, automotive radar, azimuth angle resolution, neural network, deep learning.

I. INTRODUCTION

An automotive radar is one of the most important sensors for the detection and recognition of objects around a vehicle in an autonomous driving system, along with a camera and a lidar [1-3]. A radar is a radio wave sensor that transmits a signal toward a target, receives a signal reflected by the target, and measures its delay time to obtain a distance from the radar to the target. In order to acquire a 2-D radar image composed of a range axis and an azimuth axis, a technique of obtaining a distance to a target and a technique of obtaining an azimuth angle of a target are required.

In this paper, FMCW technique is used to measure the distance of the target, and MIMO technique is used to obtain the azimuth angle of the target. In MIMO FMCW radar, the distance resolution is determined by bandwidth, pulse length, FMCW frequency slope, ADC sampling rate, etc. The azimuth angle resolution is determined by the number of Tx and Rx antennas, antenna spacing, etc. When all available bandwidths are used in the 77-81 GHz band, then the distance resolution can meet up to 3.75 cm. However, in the case of the azimuth angle resolution, since the number of antennas cannot be freely increased without restriction to improve the resolution, a study on the DOA algorithm for improving the azimuth angle resolution is required.

In this paper, the signal model of MIMO FMCW radar is introduced in section 2, and then the method for improving the azimuth angle resolution is described in section 3. Section 4 describes the verification process of the proposed method.

II. MIMO-FMCW RADAR

In the case of an FMCW radar, a triangular wave or a sawtooth wave is generally used. In this paper, a sawtooth type signal is used. After transmitting the sawtooth signal toward the target, mixing the transmitted signal and the signal reflected by the target can obtain a beat signal, and the frequency of the beat signal is determined by the distance of the target. Hence, the frequency domain obtained by Fourier transform of the beat signal becomes the range domain of the target. The 2D target scattering signal model using the MIMO FMCW radar is expressed as follows.

$$s(n,m) = \sum_{k=1}^{K} A_k e^{j2\pi\left(\frac{BW2}{T_c c} r_k\right) t_n} e^{-2\pi\left(2\frac{f}{c}\sin\theta_k\right) d_m}. \quad (1)$$

In (1), K is a total number of scatterer, T_c is a pulse duration, r_k and θ_k is range and azimuth angle at kth scatterer, respectively.

The target scattering signal model expressed in (1) has an advantage of easily obtaining range and azimuth angle using a 2-D Fourier transform. However, the scattering signal model of the target expressed in equation (1) is assuming that the target does not move during one sawtooth period and the total length of the antenna array is short enough that the target is observed with the same azimuth angle in each antenna element. Thus, when extracting target range and azimuth angle information from the target scattering signal model of equation (1), it should be noted that it is an observation environment that satisfies the previous assumptions, and a new target scattering signal model is required in an observation environment outside these assumptions. In the case of an automotive radar, the period of the sawtooth wave is determined in consideration of the moving speed of the vehicle, and a target is observed in sufficiently far away from radar with a small antenna array. Therefore, the signal model of equation (1) can be used because the signal is measured in a situation where these assumptions are satisfied. Range resolution and azimuth angle resolution are expressed as follows [4].

$$\Delta R = \frac{c}{2BW}, \quad (2)$$

$$\Delta\theta = \frac{\lambda}{2Md}. \quad (3)$$

In equation (3), λ is the wavelength of the radar signal, d is the separation distance between antenna elements.

Since the range resolution is determined by the bandwidth, it is possible to achieve a high resolution distance resolution by using a wide bandwidth. However, in the case of azimuth angle resolution, 120 antenna elements are required to reach 1° azimuth angle resolution [5]. When an array antenna consisting of a large number of antenna elements is actually constructed to secure azimuth angle resolution, the designer faces a design problem of a module controlling a large number of antennas, and a calibration problem of phase error and loss caused by the antenna line. Therefore, in this paper, MIMO technique is used to form multiple virtual antennas with fewer Tx and Rx antennas to maximize azimuth angle resolution.

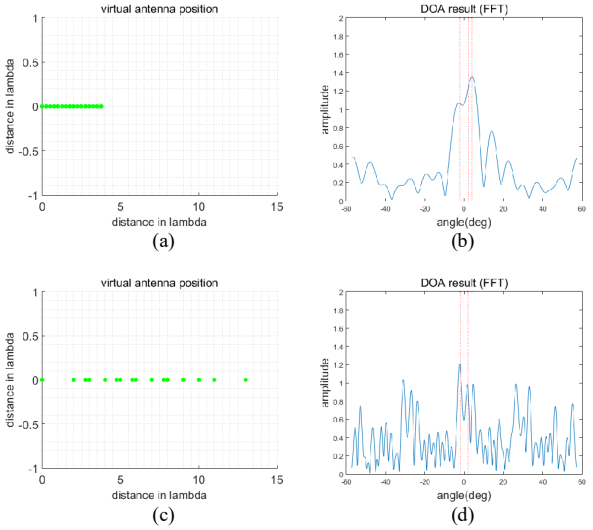

Fig. 1. 1-D DOA performance comparison using uniform and non-uniform virtual array (a) uniform virtual array geometry (b) DOA results with uniform virtual array (c) non-uniform virtual array geometry (d) DOA results with non-uniform virtual array

When using MIMO technique, virtual antennas can be formed by multiplying the number of Tx antennas by the number of Rx antennas. When 11 Tx antennas and 11 Rx antennas are used, 121 virtual antennas can be formed, and a total of 22 Tx and Rx antennas can achieve 1° azimuth angle resolution.

III. Azimuth Resolution Improvement Method

In general, algorithms using covariance matrices such as MUSIC and ESPRIT are good candidates for improving azimuth angle resolution. However, these algorithms require long-term observation of a static target in order to obtain a high quality covariance matrix because the covariance matrix determines the imaging performance [6]. However, in the case of an automotive radar, it is difficult to expect excellent performance for algorithms using a covariance matrix because the vehicle-mounted radar continuously receives signals for rapidly changing targets while moving. In addition, it is difficult to adopt those algorithm for real-time image acquisition, since formation of a covariance matrix for image acquisition, eigen value decomposition, search and estimation all require a high amount of computation. Therefore, this paper proposes a method of acquiring the azimuth angle by introducing an array antenna with non-uniform spacing and using a network that has been previously learned.

According to equation (3), the azimuth angle resolution is improved as the length of the antenna array increases. Thus, in order to achieve a higher azimuth angle resolution with using the same number of virtual antennas, the separation distance between antenna elements need to increase. However, if the virtual antennas are placed at equal intervals, aliasing will occur and the observable azimuth range will be reduced [7, 8]. Therefore, it is necessary to place virtual antennas at non-uniform intervals to achieve high resolution while avoiding aliasing.

Fig. 1 shows the placement of virtual antennas at uniform intervals and the placement of virtual antennas at non-uniform intervals, and the results of azimuth angle acquisition by fast Fourier transform (FFT). In both cases, the same number of virtual antennas were used, and when comparing the results of

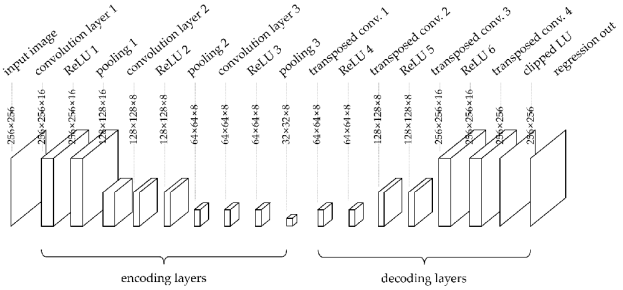

Fig. 2. Neural network structure used for radar imaging

obtaining the azimuth angle using the Fourier transform, when the antenna array length was increased using the non-uniform virtual antenna, it was confirmed that a higher resolution azimuth angle was obtained. However, as the antenna array was increased, there were regions that could not be sampled between the virtual antennas, so it can be seen that the side lobe level increased significantly in the Fourier transformed azimuth angle domain. Thus, in this paper, a previously learned neural network is use to suppress the side lobe level and obtain the azimuth angle.

Recently, deep learning technology has been widely used to remove unwanted noise signals from images. The side lobe effect caused by using a non-uniform array can be eliminated by using deep learning technology, although different from the noise signal. In order to train a neural network that performs the function of removing side lobes from an image, radar signal data is required. For randomly placed targets, radar signal data using a uniform array and radar signal data using a non-uniform array were obtained using simulation. In this paper, a radar with 4 Tx antennas and 4 Rx antennas is assumed. In the case of radar with uniform array, 64 uniform radar arrays were assumed and radar signals were acquired using simulation. For a radar with a non-uniform array, it was assumed to have 16 non-uniform virtual antenna elements out of 64 uniform virtual arrays. For the randomly generated target, the radar signal generated through the non-uniform array and the radar signal generated through the uniform array corresponded to training data set and response data set, respectively. These training data sets and response data sets were used for neural network learning. A typical neural network was used for the learning as shown in Fig. 2. Thus, if a radar image obtained with a non-uniform array is input to a trained neural network, the image acquired using a uniform array will be output.

IV. Experimental Results

To train the network, 5000 models composed of point targets located at random position were used. For each target model, radar signals obtained using 16 non-uniform arrays were generated as simulations and used as training data. And radar signals obtained using 64 uniform arrays were generated by simulation and used as response data. When generating a radar signal, the SNR was set to 9dB. The epoch was set to 100.

In order to verify the proposed method, simulation experiments and measurement experiments were performed respectively. First, in order to verify the proposed method using simulation, radar receiving signals for two scenarios were generated by point targets as shown in Fig. 3(a) and Fig. 3(e). In this experiment, since a radar system having 4 Tx

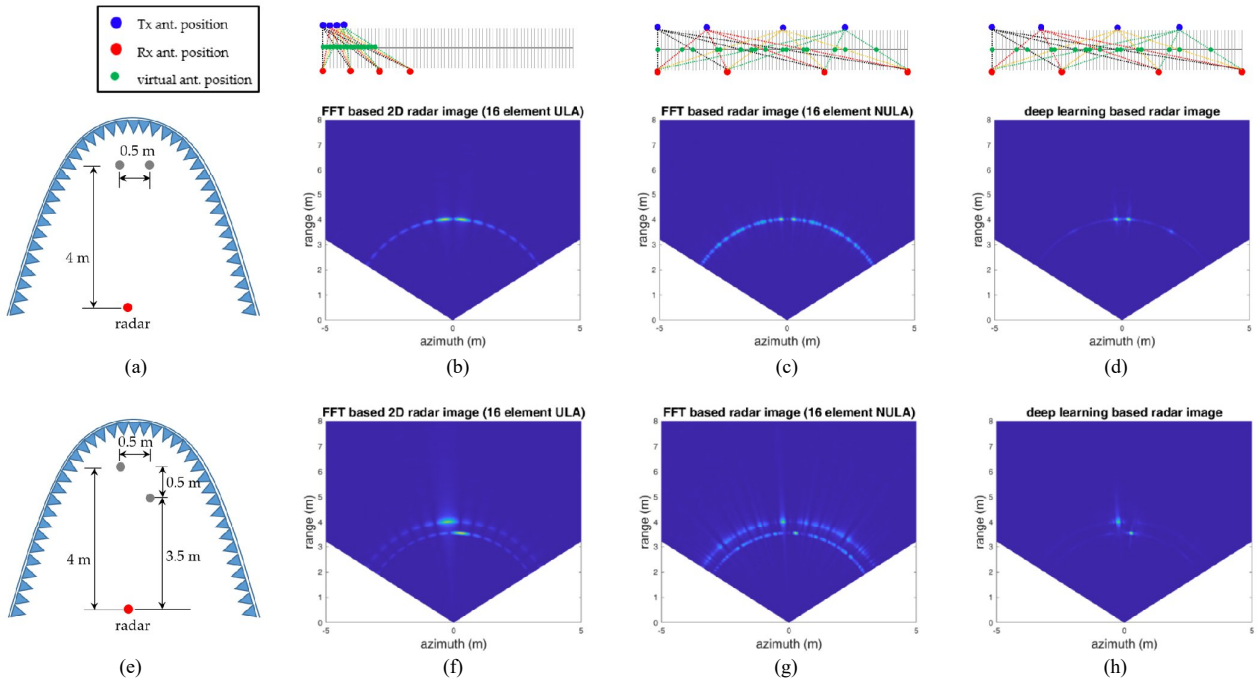

Fig. 3. radar imaging with simulated data (a) schematic of scenario 1 (b) uniform array (c) Non-uniform array with FFT (d) Non-uniform array with deep learning (e) schematic of scenario 2 (f) uniform array (g) Non-uniform array with FFT (h) Non-uniform array with deep learning

antennas and 4 Rx antennas is assumed, radar signals using 16 uniform arrays and radar signals using 16 non-uniform arrays are generated. For the both scenarios, the 2D radar images obtained by applying the FFT technique to the signals obtained using 16 uniform arrays are shown in Fig. 3(b) and Fig. 3(f). And, 2D radar images obtained by applying FFT to radar signals using 16 non-uniform arrays are shown in Fig. 3(c) and Fig. 3(g). It can be seen that the azimuth resolution is improved when the antenna aperture length is increased by arranging the same number of virtual antennas non-uniformly. However, as shown in Fig. 1, it can be seen that the quality of the image deteriorates due to the increase in the side lobe level as the non-uniform array is used. Meanwhile, the radar image obtained by the deep learning technique using the previously learned neural network is shown in Fig. 3(d) and Fig. (h). It can be seen that deep learning approach effectively removes side lobes caused by non-uniform arrays. In deep learning based image results, the range resolution is the same, but the azimuth resolution is improved 4 times by increasing the antenna aperture length 4 times using a non-uniform array.

Measurement experiments were also conducted to verify the proposed algorithm. Fig. 4(a) and Fig. 4(e) show the measurement environment for two scenarios. Two corner reflectors with a length of 18.1 cm were located as shown in Fig. 4 to measure scattering signals. The corner reflectors were placed in the same point target location as the simulation in Fig. 3. A TI AWR 1243 radar was used in the experiment. The AWR 1243 radar has 3 Tx antennas and 4 Rx antennas to form a total of 12 virtual antennas, but in the experiment, only 2 Tx antennas were activated and only 8 virtual antennas were used. The reason is that one of the Tx antennas is located in a position away from the linear arrangement to obtain an elevation angle, so this antenna was deactivated to the experiment. In order to verify the proposed method, a radar using virtual antennas arranged at non-uniform intervals is required, but the radar manufacturer does not provide a radar module of the type required in this experiment. Thus, in this experiment, in order to obtain a signal measured in a non-uniform virtual antenna, a method of selecting a virtual antenna element having a non-uniform spacing from a signal measured with a uniformly spaced virtual antenna was used. The AWR 1243 radar was horizontally moved 8 times, and the scattering signal was measured 8 times against a static target. Since 8 measurements were performed with 8 virtual antennas, it can be composed of scattered signals measured in 64 uniformly spaced virtual antenna coordinates in a linear fashion. On the other hand, if 4 Tx antennas and 4 Rx antennas are used as shown in Fig. 4, a total of 16 virtual antennas are generated, and when the Tx antenna and the Rx antenna are arranged as shown in the figure, 16 uneven virtual antennas can be formed. Of the 64 uniformly spaced virtual antennas previously measured, only signals corresponding to the 16 virtual antenna elements determined in Fig. 4 were selected and imitated as a measurement signal of a non-uniform virtual antenna. The 16 virtual antennas shown in Fig. 4 are designed so that the total length of the antenna array is equal to 64 uniformly spaced virtual antennas, and no duplicate virtual antennas are generated. In addition, the positions of the Tx antenna and the Rx antenna were determined by adjusting so that the distance between the specific virtual antennas is not too large or the virtual antennas are not concentrated in a specific area. For the both measurement scenarios, the 2D radar images obtained by FFT is shown in Fig. 4(b) and Fig. 4(f). The imaging result for the measurement signal is similar to that of the simulation signal. However, the radar image of the measurement signal contains weakly the reflected signal by the absorber, and contains a slight position error between the point target used in the simulation signal and the position of the actual corner reflector. However, the imaging results of the simulation signal and the measurement signal are still similar. Therefore, the desired result can be expected to be obtained even if the previously learned neural network is

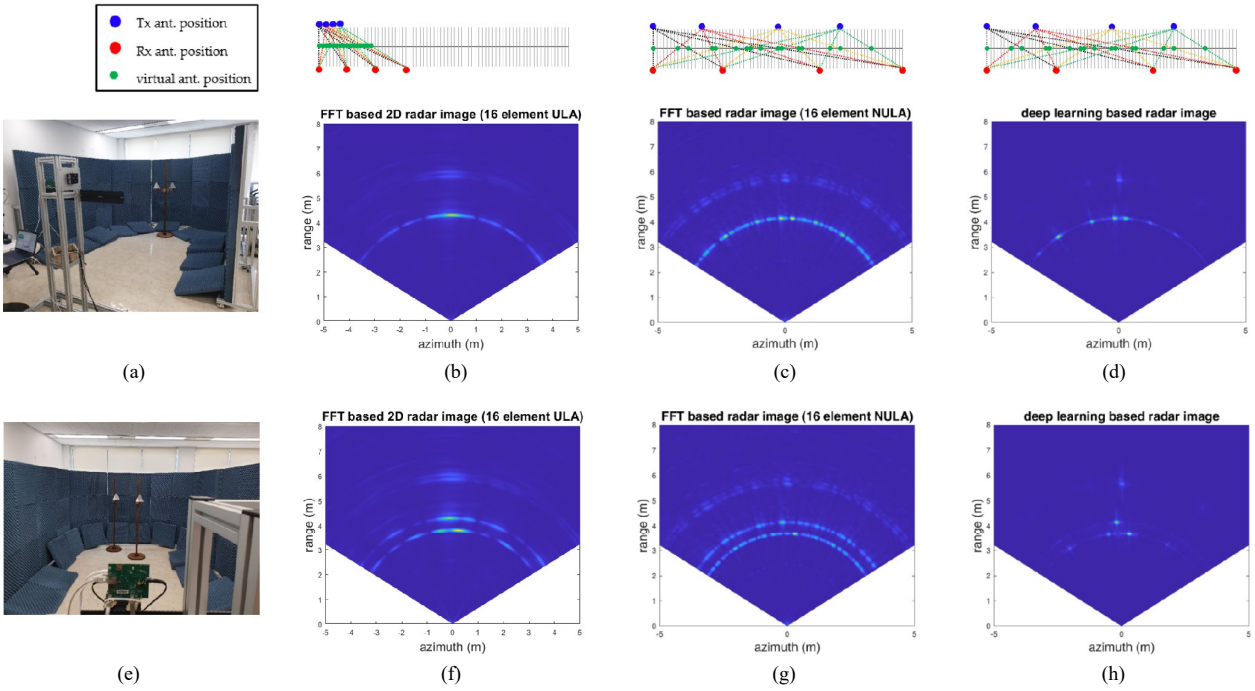

Fig. 4. radar imaging with measured data (a) schematic of scenario 1 (b) uniform array (c) Non-uniform array with FFT (d) Non-uniform array with deep learning (e) schematic of scenario 2 (f) uniform array (g) Non-uniform array with FFT (h) Non-uniform array with deep learning

applied to the measured signal in the same way to apply it to the preceding simulation signal. In Fig. 4(c) and Fig. 4(g), 2D radar images obtained by applying FFT to radar signals using 16 non-uniform arrays are shown. In Fig. 4(d) and Fig. (h), the radar image obtained by the deep learning technique using the previously learned neural network is shown. In the experiment using the measurement signal, it can be seen that the resolution can be improved by using a non-uniform array, and the side lobe caused by this can be reduced by deep learning technology.

Unlike the case of using the simulation signal, it can be seen that the results using the measurement signal include scattering points such as some ghost targets. It is presumed that this is because the measurement signal is measured by moving the radar manually, rather than using a radar system composed of one antenna array. Therefore, it is expected that better imaging results will be obtained if a single radar module including a non-uniform array antenna is used.

V. Conclusion

This paper proposed a method for improving the azimuth angle resolution of a radar in the 77-81 GHz band. A method has been introduced to maximize azimuth angle resolution by maximizing the effective length of an array antenna using a non-uniform antenna arrangement. And to suppress an increased side lobe effect caused by the use of the non-uniform virtual array antenna, deep learning based approach were introduced in this paper. In this paper, by using a non-uniform array with 16 virtual antenna elements, we provide a quality result very similar to that of a uniform array composed of 64 antenna elements of the same antenna array length. The proposed method was verified through experiments using simulation signals and experiments using emulation signals based on measurements.

Acknowledgment

This work was supported by Electronics and Telecommunications Research Institute(ETRI) grant funded by the Korean government. [20ZH1100, Study on 3D communication technology for hyper-connectivity.]

References

[1] M. Steinhauer, H. O. Ruob, H. Irion, W. Menzel, "Millimeter-wave-radar sensor based on a transceiver array for automotive applications," *IEEE Transaction on Microwave Theory and Techniques*, vol. 56, no. 2, pp. 261-269, 2008.

[2] R. Feger, A. Stelzer, "A 77-GHz FMCW MIMO radar based on an SiGe single-chip transceiver," *IEEE Transaction on Microwave Theory and Techniques*, vol. 57, no. 5, pp. 1020-1035, 2009.

[3] J. Xu, W. Hong, H. Zhang, G. Wang, Z. H. Jiang, " An array antenna for both long- and medium-range 77 GHz asutomotive radar applications," *IEEE Transaction on Antennas and Propagation*, vol. 65, no. 12, pp. 7207-7216, 2017.

[4] C. Pfeffer, R. Feger, C. Wagner, A. Stelzer, "FMCW MIMO radar system for frequency-division multiple TX-beamforming," *IEEE Transaction on Microwave Theory and Techniques*, vol. 62, no. 12, pp. 4262-4274, 2013.

[5] A. Ganis, E. M. Navarro, V. Ziegler, "A portable 3-D imaging FMCW MIMO radar demonstration with a 24x24 antenna array for medium-range application," *IEEE Transaction on Geoscience and Remote Sensing*, vol. 56, no. 1, pp. 298-312, 2018.

[6] J. M. Eckhardt, N. Joram, A. Figueroa, B. Lindner, F. Ellinger, "FMCW mulitiple-input multiple-output radar with iterative adaptive beamforming," *IET Radar Sonar and Navigation*, vol. 12, pp. 1187-1195, 2018.

[7] D. Bleh, M. Rosch, O. Ambacher, "W-band time-domain multiplexing FMCW MIMO radar for far-field 3-D imaging," *IEEE Transaction on Microwave Theory and Techniques*, vol. 65, no. 9, pp. 3474-3484, 2017.

[8] Z. Peng, C. Li, "A portable K-band 3-D MIMO radar with nonuniform spaced array for short-range localization," *IEEE Transaction on Microwave Theory and Techniques*, vol. 66, no. 11, pp. 5075-5086, 2018.